

Wave Following Control Based on Robust Adaptive Method and ADRC for a Flying Boat

Huan Du, Guoliang Fan, Yinggu Zhu, Jianqiang Yi

Abstract—The flying boat, as one of the general aviation aircraft, can take off and land from water, which is widely used in terms of both military and civilian field. It is affected by aerodynamic force and hydrodynamic force, making the controller design a difficult problem. To operate in different wave conditions, the flying boats should avoid dynamic instability phenomena and keep good sea-keeping ability. In this paper, a nonlinear controller is introduced based on robust adaptive method and ADRC (Active Disturbance Rejection Control), weakening the wave influence and achieving the wave following control. Finally, the simulation results in three water conditions demonstrate that the proposed controller can improve the anti-waves capability and reduce the impact from water.

I. INTRODUCTION

COMPARED with other flying vehicles, flying boats have some unique advantages because of its water movements and water resides operational capability. However, autonomous takeoff and landing control is still a challenging problem due to the uncertainty that comes from the sea waves. In addition, dynamic instability phenomena still exists, such as porpoising, which refers to the longitudinal coupling among heave, pitch angle and speed. Therefore, it's necessary to design high-performance controllers to improve the flying boats anti-waves capability and solve the motion instability problem.

Although flying boats have been developed and researched for hundreds of years, there is no systematic and comprehensive public literature on controller designing methods except limited studies. Eubank [1] [2] adopted traditional decoupled proportional-derivative control laws with a mode-based gain scheduling scheme for the flying fish unmanned aerial system. Zhu et al [3] [4] proposed a compound controller (active-disturbance rejection controller and dynamic inversion methods) based on the mathematical model of a flying boat. Moreover, control methods of high-speed planning vessel can be used for reference since dynamic characteristics of a flying boat are similar to it. Xi [5] designed a nonlinear controller based on the feedback linearization method to avoid porpoising of planning boat at high speeds. Gao [6] used Fuzzy-Neural Networks to control planning vessel's attitude and reduce the vessel's roll.

This work was supported by the National Natural Science Foundation of China (No.61273336) and the Innovation Method Fund of China (No.2012IM010200).

Huan Du is with the Institute of Automation, Chinese Academy of Sciences, Beijing, China (e-mail: huan.du@ia.ac.cn).

Guoliang Fan, Yinggu Zhu and Jianqiang Yi are with the Institute of Automation, Chinese Academy of Sciences, Beijing, China (e-mail: guoliang.fan@ia.ac.cn, yinggu.zhu@ia.ac.cn, jianqiang.yi@ia.ac.cn).

Furthermore, as special airplanes, the abundant research achievements on flight control have guiding significances for developing flying boat controllers. Scientists and engineers had introduced numerous effective control methods to improve the airplane performances, such as nonlinear control, adaptive control, intelligent control and so on [7] [8] [9].

Recently, the longitudinal nonlinear mathematical model combined aerodynamic and hydrodynamic effects has been developed by Zhu et al for a flying boat [3]. However, complex model with input-output cross-coupling, strong nonlinearities and external disturbances makes it difficult to design controllers. Moreover, the inaccuracy of hydrodynamic estimation intensifies the parametrical uncertainties. During takeoff from the water, the flying boats will suffer from a set of superimposed waves with different amplitudes and periods, which requires that the controllers should be able to predict the waves' influences and achieve the wave following control.

Based on the previous work, this paper proposes a new control approach applying robust adaptive method and ADRC, which guarantees the stability and seakeeping ability for flying boats. The control system utilizes double loop scheme to track related command in order to keep the flying boats safe in different wave conditions.

The organization of this paper is as follows: In section 2, the nonlinear mathematical model is briefly described and the calculation method of hydrodynamic is given. In section 3, the controller design based on robust adaptive method and ADRC is introduced. The simulation results show the performances of the controller in three wave conditions in section 4. Finally, the concluding remarks are summarized in section 5.

II. NONLINEAR MODEL OF THE FLYING BOAT

In this section, three coordinate systems are defined firstly. Then, combining Newton's law of motion and Savitsky's semi-empirical method [10], a longitudinal mathematical model is derived for the flying boat [3].

A. Coordinates Definition

A right-handed coordinate system is defined in Fig.1.

- Earth-fixed coordinate system with X_e, Y_e, Z_e axes, with the X_e axis lying in the undisturbed water surface pointing in the direction of the forward speed.

- Steady-translating coordinate system with X_s, Y_s, Z_s axes, with the X_s axis lying in the undisturbed water surface pointing in the direction of the forward speed and travelling with a given constant speed.

- Body-fixed coordinate system with X_b, Y_b, Z_b axes, with the origin in the centre of gravity (CG) of the ship and of which the X_b axis is the longitudinal axis pointing forward.

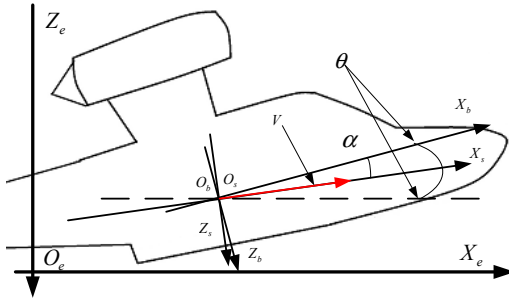


Fig. 1. The coordinate systems
where α = angle of attack; θ = angle of pitch.

B. Longitudinal Mathematical Model

According to the longitudinal mathematical model developed by Zhu et al [3], the forces acting on a flying boat can be categorized into weight, forces from water, aerodynamic forces, and engine thrust (Fig. 2).

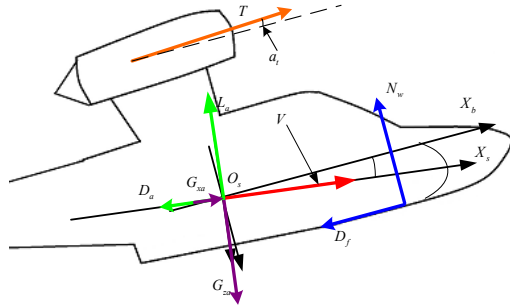


Fig. 2. The forces acting on the flying boat

The nonlinear longitudinal dynamic model of the flying boat is represented by

$$\left. \begin{array}{l} m\dot{V} = T \cos(\alpha + \alpha_t) - D_a - N_w \sin \alpha - D_f \cdot \cos \alpha + G_{xa} \\ mV\dot{\alpha} = mVq - T \sin(\alpha + \alpha_t) - L_a - N_w \cdot \cos \alpha + D_f \cdot \sin \alpha + G_{za} \\ I_y \dot{q} = M_a + M_w + M_T \\ \dot{\theta} = q \\ \dot{x}_g = u \cos \theta + w \sin \theta \\ \dot{z}_g = -u \sin \theta + w \cos \theta \end{array} \right\} \quad (1)$$

where

- m = the mass of the flying boat;
- V = the speed of the flying boat;
- T = the thrust of engine;
- α_t = the angle between engine force and X_b ;
- N_w = the water pressure normal to the bottom;
- L_a = the aerodynamic lift;
- D_a = the aerodynamic drag;
- D_f = the water friction along the bottom;
- u, w = the speed components of the flying boat along X_b, Z_b ,
- $u = V \cos \alpha, w = V \sin \alpha$;
- q = the pitch angular rate;

I_y = the flying boat's moment of inertia about Y_b ;
 x_g, z_g = the position of the flying boat along X_e, Z_e ;
 M_a, M_w, M_T = the total pitching moment from air, water and engine;
 G_{xa}, G_{za} = the gravity along X_s, Z_s ,
 $G_{xa} = mg(-\cos \alpha \sin \theta + \sin \alpha \cos \theta)$,
 $G_{za} = mg(\sin \alpha \sin \theta + \cos \alpha \cos \theta)$;
 g = acceleration due to gravity.

The state vector of the longitudinal dynamic model is

$$X = [V \ \alpha \ q \ \theta \ x_g \ z_g]^T$$

The engine throttle δ_{th} and the elevator deflection δ_e form the vector of control variables

$$u = [\delta_{th} \ \delta_e]^T$$

C. Water Forces

Savitsky's semi-empirical method of planning hulls motion predication can be applied to calculate water forces of the flying boat [10]. The effective mean wetted length-beam ratio, λ , plays an important role in water forces estimate.

Water lift of the flying boat is calculated by following formulas:

$$N_w = 0.5\rho V^2 B^2 C_{L\beta} \quad (2)$$

$$C_{L\beta} = C_{L0} - 0.0065\beta C_{L0}^{0.6} \quad (3)$$

when $C_v \leq 10$

$$C_{L0} = \theta^{1.1}(0.012\lambda^{0.5} + 0.0055\lambda^{2.5} / C_v^2) \quad (4)$$

when $C_v > 10$

$$C_{L0} = 0.012\lambda^{0.5}\theta^{1.1} \quad (5)$$

where

$C_v = V / \sqrt{gB}$ is the speed coefficient;

B = the beam length;

C_{L0} = lift coefficient for a zero deadrise surface;

$C_{L\beta}$ = lift coefficient for surface with constant deadrise of β ;

ρ = water density.

The water friction is calculated by following equations:

$$D_f = 0.5C_f \rho V_1^2 \lambda B^2 / \cos \beta \quad (6)$$

$$C_f = 0.072 / \log_{10}(Re)^{2.58} \quad (7)$$

$$V_1 = V(1 - 2p_d / (\rho V^2))^{0.5} \quad (8)$$

$$p_d = N_w / (\lambda B^2 \cos \theta) \quad (9)$$

where

C_f = Schoenherr turbulent friction coefficient;

V_1 = the average bottom velocity;

R_e = Reynolds number;

p_d = the average dynamic pressure.

The center of water pressure of the flying boat can be expressed as follows:

$$l_p = \lambda B(0.75 - \frac{1}{5.21C_v^2 / \lambda^2 + 2.39}) \quad (10)$$

where l_p is the longitudinal distance from the step point of the flying boat to the center of water pressure.

D. Aerodynamic Forces

The forces and moments acting on the longitudinal plane of the flying boat include the aerodynamic lift L_a , drag D_a and pitching moment M_a , which are calculated by the following equations:

$$\left. \begin{array}{l} Q = 0.5 \rho_a V^2 \\ L_a = QS_w C_L \\ D_a = QS_w C_D \\ M_a = QS_w c_A C_M \end{array} \right\} \quad (11)$$

where

ρ_a = air density;

Q = the dynamic pressure;

S_w = the wing reference area of the flying boat;

C_L = the coefficient of aerodynamic lift;

C_D = the coefficient of aerodynamic drag;

C_M = the coefficient of aerodynamic pitching moment.

III. THE CONTROLLER BASED ON ROBUST ADAPTIVE METHOD AND ADRC

A. Control Strategy

In order to design the controller effectively for the flying boat, based on the time-scale separation [9], the states are divided into three categories: fast variable q ; medium-slow variables V and α ; slow variables x_g and z_g .

Using the first three equations in Eq(1), the control system utilizes double loop scheme to track related command: The desired speed V_c and desired angle of attack α_c , are the input signals of outer loop, whose output signals are the engine throttle δ_{th} and pitch angular rate q_c . Inner loop controller is designed to follow the desired angular rate q_c and provide the elevator deflection δ_e . The specific control strategy is showed in Fig.3.

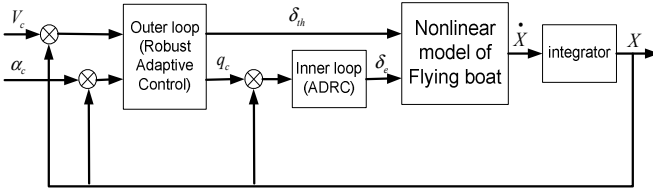


Fig. 3. The forces acting on the flying boat

B. Inner Loop Controller

Active Disturbance Rejection Control, inspired by classical PID method, absorbs the results of modern control theory and overcomes some drawbacks of PID [11], which has demonstrated its effectiveness in many industry fields [12] [13]. A typical ADRC consists of three main parts, tracking differentiator (TD), extended state observer (ESO) and non-linear state errors feedback (NLSEF). In order to improve the control performance, TD constructs a transient

profile to avoid setpoint and produces the input signals' differential. ESO can estimate the system's unmodeled dynamics and compensate the disturbances. NLSEF is used to deal with the errors between the command and the observed states to construct the feedback law.

In this paper, only ESO is used to compensate the uncertainties of the flying boat model. The third equation in Eq(1) can be rewritten as :

$$\dot{q} = f(q, \omega(t), t) + (M_a^{\delta_e} / I_y) \delta_e \quad (12)$$

where $M_a^{\delta_e}$ is the pitching moment coefficient of the elevator.

As the moments acting on the flying boat, especially hydrodynamic moment, are difficult to estimate, we regard them as unmodeled parts which are expressed by a multivariable function $f(q, \omega(t), t)$, including both system states and total disturbance. Thus, ESO can be introduced to observe the disturbance and compensate the influences of unmodeled parts. For Eq(12), ESO is represented as follows:

$$\left\{ \begin{array}{l} \varepsilon = z_1 - q \\ \dot{z}_1 = z_2 - \beta_{01} \varepsilon + (M_a^{\delta_e} / I_y) \delta_e \\ \dot{z}_2 = -\beta_{02} fal(\varepsilon, \alpha, \delta) \end{array} \right. \quad (13)$$

$$fal(\varepsilon, \alpha, \delta) = \begin{cases} |\varepsilon|^\alpha \operatorname{sgn}(\varepsilon), & |\varepsilon| > \delta, \\ \varepsilon / \delta^{1-\alpha}, & |\varepsilon| \leq \delta, \end{cases} \quad 0 < \alpha < 1, \delta > 0 \quad (14)$$

where z_1 is the estimation of the pitch angular rate q , z_2 is the extended state variable to estimate the total disturbance. β_{01} , β_{02} is the changeable parameters of ESO.

Assume that z_2 can track the function $f(q, \omega(t), t)$ well, the Eq(12) can be rewritten as:

$$\dot{q} = z_2 + (M_a^{\delta_e} / I_y) \delta_e \quad (15)$$

Replacing NLSEF by linear state error feedback, the desired closed loop dynamics model is designed as:

$$\dot{q} = k(q_c - q) = u_0 \quad (16)$$

Combining Eq(15) and (16), the elevator deflection δ_e can be obtained by

$$\delta_e = I_y / M_a^{\delta_e} \cdot [k(q_c - q) - z_2] \quad (17)$$

Fig.4 shows the diagram of inner loop controller.

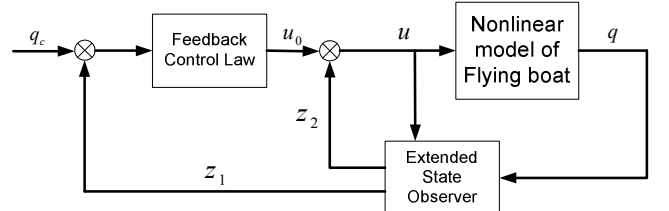


Fig. 4. The diagram of inner loop controller

C. Outer Loop Controller

Control problem statement

The first two equations in Eq(1) can be rewritten as:

$$\dot{x} = f(x) + g(x)u \quad (18)$$

$$\begin{aligned} \mathbf{f}(\mathbf{x}) &= \begin{pmatrix} m & 0 \\ 0 & mV + L_a^{\dot{\alpha}} \end{pmatrix}^{-1} \begin{pmatrix} G_{xa} - D_{a0} - N_w \sin \alpha - D_w \cos \alpha \\ G_{za} - L_{a0} - N_w \cos \alpha + D_w \sin \alpha - L_a^{\delta_e} \delta_e \end{pmatrix} \\ \mathbf{g}(\mathbf{x}) &= \begin{pmatrix} m & 0 \\ 0 & mV + L_a^{\dot{\alpha}} \end{pmatrix}^{-1} \begin{pmatrix} C_T^{\delta_h} \cos(\alpha + \alpha_t) - D_a^{\delta_h} & 0 \\ -C_T^{\delta_h} \sin(\alpha + \alpha_t) - L_a^{\delta_h} & mV \end{pmatrix} \\ \mathbf{x} &= \begin{pmatrix} V \\ \alpha \end{pmatrix} \quad \mathbf{u} = \begin{pmatrix} \delta_h \\ q_c \end{pmatrix} \end{aligned} \quad (19)$$

where $L_{a0}, D_{a0}, L_a^{\dot{\alpha}}, L_a^{\delta_h}, D_a^{\delta_h}$ are aerodynamic coefficient of the flying boat, $C_T^{\delta_h}$ is the coefficient of engine throttle. For convenience, we define $\mathbf{f}(\mathbf{x}), \mathbf{g}(\mathbf{x}), \mathbf{u}$ as :

$$\mathbf{f}(\mathbf{x}) = \begin{pmatrix} f_1(\mathbf{x}) \\ f_2(\mathbf{x}) \end{pmatrix} \quad \mathbf{g}(\mathbf{x}) = \begin{pmatrix} g_{11}(\mathbf{x}) & g_{12}(\mathbf{x}) \\ g_{21}(\mathbf{x}) & g_{22}(\mathbf{x}) \end{pmatrix} \quad \mathbf{u} = \begin{pmatrix} u_1 \\ u_2 \end{pmatrix} \quad (20)$$

Eq(18) is a typical MIMO nonlinear system. The objective is to design a controller to track the desired state vector $\mathbf{x}_c = [V_c \ \alpha_c]^T$, that is, the tracking error can be attenuated to a small residual set as close as possible.

The tracking error is given as follows:

$$\mathbf{e} = [e_V \ e_\alpha]^T, (e_V = V - V_c, e_\alpha = \alpha - \alpha_c) \quad (21)$$

We define the following error metric:

$$\begin{aligned} \mathbf{S} &= [S_V \ S_\alpha]^T \\ &= \begin{pmatrix} e_V + \lambda_V \int_0^t e_V d\tau \\ e_\alpha + \lambda_\alpha \int_0^t e_\alpha d\tau \end{pmatrix} \end{aligned} \quad (22)$$

where $\lambda_V, \lambda_\alpha$ are positive constants to be selected.

Combining Eq(18), the time derivative of \mathbf{S} can be expressed as:

$$\begin{aligned} \dot{\mathbf{S}} &= [\dot{S}_V \ \dot{S}_\alpha]^T = \begin{pmatrix} \dot{e}_V + \lambda_V e_V \\ \dot{e}_\alpha + \lambda_\alpha e_\alpha \end{pmatrix} \\ &= \begin{pmatrix} f_1(\mathbf{x}) \\ f_2(\mathbf{x}) \end{pmatrix} + \begin{pmatrix} V_1(t) \\ V_2(t) \end{pmatrix} + \begin{pmatrix} g_{11}(\mathbf{x}) & g_{12}(\mathbf{x}) \\ g_{21}(\mathbf{x}) & g_{22}(\mathbf{x}) \end{pmatrix} \begin{pmatrix} u_1 \\ u_2 \end{pmatrix} \end{aligned} \quad (23)$$

where,

$$\begin{cases} V_1(t) = -\dot{V}_c + \lambda_V e_V \\ V_2(t) = -\dot{\alpha}_c + \lambda_\alpha e_\alpha \end{cases} \quad (24)$$

Eq(23) can be written in the compact form:

$$\dot{\mathbf{S}} = \mathbf{f}(\mathbf{x}) + \mathbf{v}(t) + \mathbf{g}(\mathbf{x})\mathbf{u} \quad (25)$$

Assume that $\mathbf{f}(\mathbf{x}), \mathbf{g}(\mathbf{x})$ are completely known and $\mathbf{g}(\mathbf{x})$ is invertible, the control law can be designed as:

$$\mathbf{u} = \mathbf{g}^{-1}(\mathbf{x})[-\mathbf{f}(\mathbf{x}) - \mathbf{v}(t) - \mathbf{KS}] \quad (26)$$

where $\mathbf{K} = \text{diag}(k_V, k_\alpha), k_V, k_\alpha > 0$

which guarantees that $\lim_{t \rightarrow \infty} \|\mathbf{S}\| = 0$.

According to [14] [15], the control law can be rewritten as:

$$\mathbf{u} = \frac{\mathbf{S}_e}{b(\mathbf{x})} [-k_s \|\mathbf{S}\| - \mathbf{S}_e^T \mathbf{f}(\mathbf{x}) - \mathbf{S}_e^T \mathbf{v}(t)] \quad (27)$$

where $\mathbf{S}_e = \mathbf{S}/\|\mathbf{S}\|$ is the unit vector, $b(\mathbf{x})$ is called the gain function. For square matrix $\mathbf{g}(\mathbf{x})$ satisfying certain assumption, we have $\mathbf{S}_e^T \mathbf{g}(\mathbf{x}) \mathbf{S}_e = b(\mathbf{x}) \|\mathbf{S}_e\|^2 = b(\mathbf{x})$. Thus,

using Eq(27), the calculation of the inverse of $\mathbf{g}(\mathbf{x})$ can be avoided.

Neural network approximation

In the control law (27), $\mathbf{f}(\mathbf{x})$ and $b(\mathbf{x})$ are assumed to be completely known. However, for the flying boats, $\mathbf{f}(\mathbf{x})$ and $b(\mathbf{x})$ are difficult to be expressed accurately due to the strong nonlinearities and uncertainties of the wave conditions. In this paper, radial basis-function (RBF) neural networks are used to approximate the unknown function [14] [17]. It has been proved that RBF neural networks can approximate any nonlinear function to arbitrary accuracy. Fig.5 shows the structure of RBF neural networks.

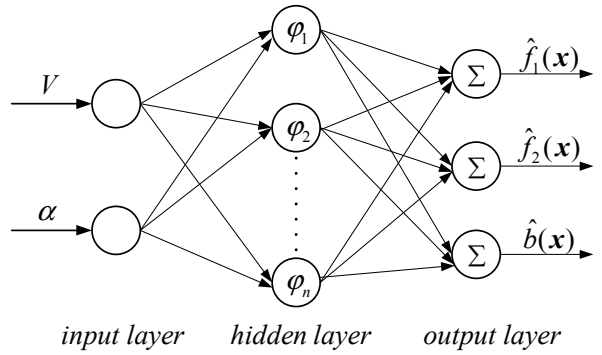


Fig. 5. The structure of RBF neural networks

The neural networks include three layers: V and α are used as the input layer of the networks, whose output layer is the approximation of $\mathbf{f}(\mathbf{x})$ and $b(\mathbf{x})$. Gauss function is selected as the radial basis function, which is expressed in the following form:

$$\phi_i = \exp\left(-\frac{\|\mathbf{x} - \mathbf{c}_i\|^2}{2\sigma_i^2}\right) \quad i = 1, 2, \dots, n \quad (28)$$

where n represents the number of nodes in the hidden layer.

$\mathbf{c}_i = [c_{iV} \ c_{i\alpha}]^T$ is the center vector of the i th node. $\sigma = [\sigma_1 \ \sigma_2 \ \dots \ \sigma_n]^T$ is the width vector of the neural networks.

$\mathbf{f}(\mathbf{x})$ and $b(\mathbf{x})$ are approximated as follows:

$$\begin{aligned} f_i(\mathbf{x}) &\approx \hat{f}_i(\mathbf{x} | \boldsymbol{\theta}_{f_i}) = \boldsymbol{\theta}_{f_i}^T \boldsymbol{\phi}(\mathbf{x}) \quad i = 1, 2 \\ b(\mathbf{x}) &\approx \hat{b}(\mathbf{x} | \boldsymbol{\theta}_b) = \boldsymbol{\theta}_b^T \boldsymbol{\phi}(\mathbf{x}) \end{aligned} \quad (29)$$

where $\boldsymbol{\theta}_{f_i}, \boldsymbol{\theta}_b$ are weight vectors, $\boldsymbol{\phi}(\mathbf{x}) = [\phi_1(\mathbf{x}), \dots, \phi_n(\mathbf{x})]$.

We define the parameters of the best function approximation as:

$$\begin{aligned} \boldsymbol{\theta}_{f_i}^* &= \arg \min_{\boldsymbol{\theta}_{f_i} \in \Omega_{f_i}} [\sup |f_i(\mathbf{x}) - \hat{f}_i(\mathbf{x} | \boldsymbol{\theta}_{f_i})|] \\ \boldsymbol{\theta}_b^* &= \arg \min_{\boldsymbol{\theta}_b \in \Omega_b} [\sup |b(\mathbf{x}) - \hat{b}(\mathbf{x} | \boldsymbol{\theta}_b)|] \end{aligned} \quad (30)$$

where Ω_{f_i} and Ω_b are constraint sets for $\boldsymbol{\theta}_{f_i}$ and $\boldsymbol{\theta}_b$.

Let

$$\begin{aligned} \tilde{\boldsymbol{\theta}}_{f_i} &= \boldsymbol{\theta}_{f_i} - \boldsymbol{\theta}_{f_i}^* \quad i = 1, 2 \\ \tilde{\boldsymbol{\theta}}_b &= \boldsymbol{\theta}_b - \boldsymbol{\theta}_b^* \end{aligned} \quad (31)$$

Then the minimum approximation errors can be written as:

$$\begin{aligned}\hat{f}_i(\mathbf{x}) - \hat{f}_i^*(\mathbf{x}) &= \tilde{\boldsymbol{\theta}}_{f_i}^T \boldsymbol{\varphi}(\mathbf{x}) \quad i = 1, 2 \\ \hat{b}(\mathbf{x}) - \hat{b}^*(\mathbf{x}) &= \tilde{\boldsymbol{\theta}}_b^T \boldsymbol{\varphi}(\mathbf{x})\end{aligned}\quad (32)$$

Robust adaptive controller

Using the approximation of $f(\mathbf{x})$ and $b(\mathbf{x})$, the control law (27) can be rewritten as [14]:

$$\mathbf{u} = \frac{\mathbf{S}_e}{\hat{b}(\mathbf{x})} [-k_s \|\mathbf{S}\| - \mathbf{S}_e^T \hat{f}(\mathbf{x}) - \mathbf{S}_e^T \mathbf{v}(t)] \quad (33)$$

For simplicity, rewrite the control law (33) as:

$$\mathbf{u} = \mathbf{S}_e \mathbf{u}_0 \quad (34)$$

$$\mathbf{u}_0 = \frac{1}{\hat{b}(\mathbf{x})} [-k_s \|\mathbf{S}\| - \mathbf{S}_e^T \hat{f}(\mathbf{x}) - \mathbf{S}_e^T \mathbf{v}(t)] \quad (35)$$

The adaptive law is designed as follows:

$$\begin{cases} \dot{\boldsymbol{\theta}}_{f_1} = \gamma_{f_1} S_{\nu} \boldsymbol{\varphi}(\mathbf{x}) \\ \dot{\boldsymbol{\theta}}_{f_2} = \gamma_{f_2} S_{\alpha} \boldsymbol{\varphi}(\mathbf{x}) \\ \dot{\boldsymbol{\theta}}_b = \gamma_b \|\mathbf{S}\| \mathbf{u}_0 \boldsymbol{\varphi}(\mathbf{x}) \end{cases} \quad (36)$$

where γ_{f_1} , γ_{f_2} , γ_b are positive design parameters.

Proof:

First, define the approximation error as:

$$\boldsymbol{\omega} = \mathbf{S}_e^T [\mathbf{f}(\mathbf{x}) - \hat{\mathbf{f}}^*(\mathbf{x})] + [\mathbf{b}(\mathbf{x}) - \hat{\mathbf{b}}^*(\mathbf{x})] \mathbf{u}_0 \quad (37)$$

Consider the Lyapunov function

$$V = \frac{1}{2} (\mathbf{S}^T \mathbf{S} + \frac{1}{\gamma_{f_1}} \tilde{\boldsymbol{\theta}}_{f_1}^T \tilde{\boldsymbol{\theta}}_{f_1} + \frac{1}{\gamma_{f_2}} \tilde{\boldsymbol{\theta}}_{f_2}^T \tilde{\boldsymbol{\theta}}_{f_2} + \frac{1}{\gamma_b} \tilde{\boldsymbol{\theta}}_b^T \tilde{\boldsymbol{\theta}}_b) \quad (38)$$

Then the time derivative of V can be obtained as:

$$\dot{V} = \mathbf{S}^T \dot{\mathbf{S}} + \frac{1}{\gamma_{f_1}} \tilde{\boldsymbol{\theta}}_{f_1}^T \dot{\tilde{\boldsymbol{\theta}}}_{f_1} + \frac{1}{\gamma_{f_2}} \tilde{\boldsymbol{\theta}}_{f_2}^T \dot{\tilde{\boldsymbol{\theta}}}_{f_2} + \frac{1}{\gamma_b} \tilde{\boldsymbol{\theta}}_b^T \dot{\tilde{\boldsymbol{\theta}}}_b \quad (39)$$

Using Eq(25) and (34),

$$\begin{aligned}\mathbf{S}^T \dot{\mathbf{S}} &= \mathbf{S}^T \mathbf{f}(\mathbf{x}) + \mathbf{S}^T \mathbf{g}(\mathbf{x}) \mathbf{u} + \mathbf{S}^T \mathbf{v}(t) \\ &= \mathbf{S}^T \mathbf{f}(\mathbf{x}) + \mathbf{S}^T \mathbf{g}(\mathbf{x}) \mathbf{S}_e \mathbf{u}_0 + \mathbf{S}^T \mathbf{v}(t)\end{aligned}\quad (40)$$

According to [14], we obtain

$$\mathbf{S}_e^T \mathbf{g}(\mathbf{x}) \mathbf{S}_e = \mathbf{b}(\mathbf{x}) \|\mathbf{S}_e\|^2 = b(\mathbf{x}) \quad (41)$$

By substituting Eq(41) into (40),

$$\mathbf{S}^T \dot{\mathbf{S}} = \mathbf{S}^T \mathbf{f}(\mathbf{x}) + b(\mathbf{x}) \|\mathbf{S}\| \mathbf{u}_0 + \mathbf{S}^T \mathbf{v}(t) \quad (42)$$

$$= \mathbf{S}^T \mathbf{f}(\mathbf{x}) + \mathbf{S}^T \mathbf{v}(t) + [b(\mathbf{x}) - \hat{b}(\mathbf{x})] \|\mathbf{S}\| \mathbf{u}_0 + \hat{b}(\mathbf{x}) \|\mathbf{S}\| \mathbf{u}_0$$

Combining (35),(37) and (32), we have

$$\begin{aligned}\mathbf{S}^T \dot{\mathbf{S}} &= \mathbf{S}^T [\mathbf{f}(\mathbf{x}) - \hat{\mathbf{f}}(\mathbf{x})] + [b(\mathbf{x}) - \hat{b}(\mathbf{x})] \|\mathbf{S}\| \mathbf{u}_0 - k_s \|\mathbf{S}\|^2 \\ &= \mathbf{S}^T [\hat{\mathbf{f}}^*(\mathbf{x}) - \hat{\mathbf{f}}(\mathbf{x})] + [\hat{b}^*(\mathbf{x}) - \hat{b}(\mathbf{x})] \|\mathbf{S}\| \mathbf{u}_0 \\ &\quad - k_s \|\mathbf{S}\|^2 + \|\mathbf{S}\| \boldsymbol{\omega}\end{aligned}\quad (43)$$

$$\begin{aligned}&= -S_{\nu} \tilde{\boldsymbol{\theta}}_{f_1}^T \boldsymbol{\varphi}(\mathbf{x}) - S_{\alpha} \tilde{\boldsymbol{\theta}}_{f_2}^T \boldsymbol{\varphi}(\mathbf{x}) - \tilde{\boldsymbol{\theta}}_b^T \boldsymbol{\varphi}(\mathbf{x}) \|\mathbf{S}\| \mathbf{u}_0 \\ &\quad - k_s \|\mathbf{S}\|^2 + \|\mathbf{S}\| \boldsymbol{\omega}\end{aligned}$$

By(31), $\dot{\tilde{\boldsymbol{\theta}}}_{f_1} = \dot{\boldsymbol{\theta}}_{f_1}$, $\dot{\tilde{\boldsymbol{\theta}}}_b = \dot{\boldsymbol{\theta}}_b$, combining (36),

$$\begin{aligned}&\frac{1}{\gamma_{f_1}} \tilde{\boldsymbol{\theta}}_{f_1}^T \tilde{\boldsymbol{\theta}}_{f_1} + \frac{1}{\gamma_{f_2}} \tilde{\boldsymbol{\theta}}_{f_2}^T \tilde{\boldsymbol{\theta}}_{f_2} + \frac{1}{\gamma_b} \tilde{\boldsymbol{\theta}}_b^T \tilde{\boldsymbol{\theta}}_b = \\ &\quad S_{\nu} \tilde{\boldsymbol{\theta}}_{f_1}^T \boldsymbol{\varphi}(\mathbf{x}) + S_{\alpha} \tilde{\boldsymbol{\theta}}_{f_2}^T \boldsymbol{\varphi}(\mathbf{x}) + \tilde{\boldsymbol{\theta}}_b^T \boldsymbol{\varphi}(\mathbf{x}) \|\mathbf{S}\| \mathbf{u}_0\end{aligned}\quad (44)$$

Finally, using (39),(43) and (44),

$$\dot{V} = -k_s \|\mathbf{S}\|^2 + \|\mathbf{S}\| \boldsymbol{\omega} \quad (45)$$

The neural networks can ensure the approximation error to arbitrarily small, so we can obtain:

$$\dot{V} \leq 0 \quad (46)$$

Eq(46) suggests that the proposed controller can track the desired state well.

IV. SIMULATION RESULTS

To evaluate the performance of the proposed controller, numerical simulations are performed. Three different wave conditions are assumed for the flying boat, including calm water, regular wave and irregular wave. It's essential to trim the flying boat to equilibrium status as the initial state of each simulation. The trimmed state is: $V = 15m/s$, $\alpha = 12.42^\circ$, $q = 0rad/s$, $\theta = 12.42^\circ$, $x_g = 0m$, $z_g = -0.45m$.

For the inner controller, the design parameters are given by $\beta_{01} = 100$, $\beta_{02} = 10$, $k = 10$. For the outer controller, Gauss radial basis function is selected as:

$$\varphi_i = \exp\left(-\frac{\|\mathbf{x} - \mathbf{c}_i\|^2}{2\sigma_i^2}\right) \quad i = 1, 2, \dots, n. \quad \text{The number of nodes in}$$

the hidden layer is given as $n = 10$. We choose the center of radial base $\mathbf{c}_i = [15 + 0.2*i, 10^\circ + 0.5^\circ*i]$, the width: $\sigma_i = 5$, $i = 1, 2, \dots, 10$. The control parameters are: $\lambda_r = \lambda_\alpha = 1$, $k_s = 20$, $\gamma_{f_1} = \gamma_{f_2} = 1$, $\gamma_b = 0.1$.

The simulation results are shown from Fig.6 to Fig.8. For the height time-response, the dotted line indicates the wave surface height and the solid line indicates the height of the center of gravity. Fig.6 shows the time responses of the flying boat in calm water. It suggests that the flying boat can converge to the equilibrium state in a short time. In Fig.7, the regular wave, whose amplitude and wavelength are 0.2m, 50m, respectively, is applied in simulation. The results show that the flying boat can follow the wave surfaces very well, reducing the wave impact. In Fig.8, an irregular wave based on P-M spectrum is constructed, which can be divided into multiple regular waves with different amplitudes and wavelengths [18]. In this condition, the speed and angle of attack fluctuate in a certain range and the flying boat can track the desired state in most of time, but rough wave state makes the performance of the controller not very well. The simulation results demonstrate that the proposed controller can improve the sea-keeping ability and keep the flying boat safe in different wave conditions.

V. CONCLUSION

Complex mathematical model, strong nonlinearities and wave impact make the controller design for the flying boat a challenging problem. In this paper, a new control strategy based on robust adaptive method and ADRC is presented for the flying boat. The controller can compensate the disturbances and estimate the uncertainties of the model, improving the stability and dynamic characteristics of the flying boat. The wave following control is effective to track the surface of the waves, reduce the wave influences and strengthen the anti-waves capability. The simulation results

show that the controller has good performances in three different wave conditions (calm water, regular wave and irregular wave).

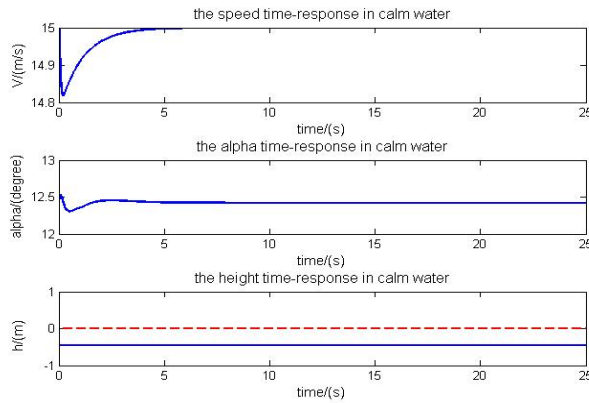


Fig. 6. The time-response in calm water

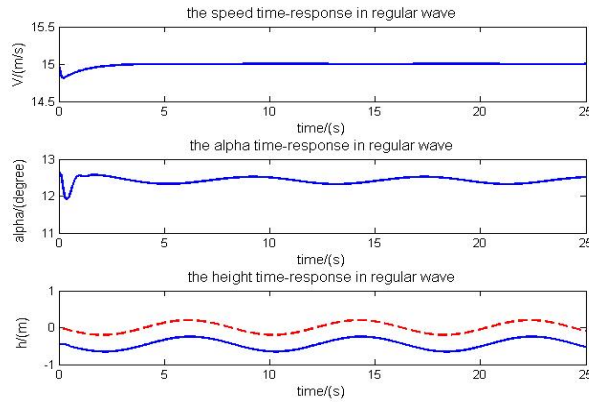


Fig. 7. The time-response in regular wave

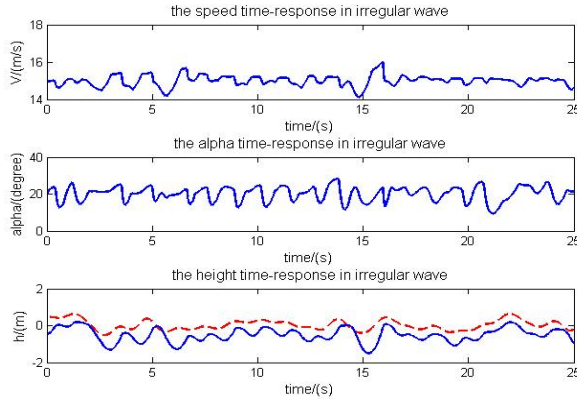


Fig. 8. The time-response in irregular wave

the 2011 IEEE International Conference on Mechatronics and Automation, pp. 2039-2044, 2011.

- [4] Y. Zhu, G. Fan and J. Yi, "Controller design for flying boats taking off from water with regular waves", *Proceedings of the 2012 IEEE International Conference on Mechatronics and Automation*, pp. 480-485, 2012.
- [5] H. Xi and J. Sun, "Nonlinear Feedback Stabilization of High-Speed Planing Vessels by A Controllable Transom Flap", *American Control Conference*, Portland, OR, Jun. 2005.
- [6] S. Gao, Q. Zhu and L. Li, "Simulation of Sliding Ship's High-speed Modeling and Attitude Control", *Journal of System Simulation*, vol. 20, no. 16, pp. 4461-4465, Aug. 2008.
- [7] S. Wu and Y. Fei, *Flight Control System (In Chinese)*, National Defense Industry Press, 2009.
- [8] S. N. Singh, M. Steinberg and R. D. DiGirolamo, "Variable Structure Robust Flight Control System for the F-14", *IEEE Trans. Aerospace and Electronic Systems*, vol. 33, no. 1, pp. 77-84, Sep. 1997.
- [9] J. Reiner, G. J. Balas and W. L. Garrard, "Flight Control Design Using Robust Dynamic Inversion and Time-scale Separation", *Automatic*, vol. 32, no. 11, pp. 1493-1504, Nov. 1996.
- [10] D. Savitsky, "Hydrodynamic Design of Planing Hulls", *Marine Technology*, vol. 1, no. 1, pp. 71-95, Oct. 1964.
- [11] J. Han, "From PID to Active Disturbance Rejection Control", *IEEE Trans. Industrial Electronics*, vol. 56, no. 3, pp. 900-906, Mar. 2009.
- [12] Y. Huang, K. Xu, J. Han and J. Lam, "Flight Control Design Using Extended State Observer and Non-smooth Feedback", *Proceedings of the 40th IEEE Conference on Decision and Control*, pp. 223-228, 2001.
- [13] B. Sun and Z. Gao, "A DSP-Based Active Disturbance Rejection Control Design for a 1-kW H-Bridge DC-DC Power Converter", *IEEE Trans. Industrial Electronics*, vol. 52, no. 5, pp. 1271-1277, Oct. 2005.
- [14] H. Xu and P. A. Ioannou, "Robust Adaptive Control for a Class of MIMO Nonlinear Systems With Guaranteed Error Bounds", *IEEE Trans. Automatic Control*, vol. 48, no. 5, pp. 728-742, May 2003.
- [15] H. Xu and M. Mirmirani, "Robust Adaptive Sliding Control for a Class of MIMO Nonlinear Systems", *AIAA Guidance, Navigation, and Control Conference and Exhibit*, Montreal, Canada, Aug. 2001, AIAA-2001-4168.
- [16] W.-S. Lin and C.-S. Chen, "Robust adaptive sliding mode control using fuzzy modeling for a class of uncertain MIMO nonlinear systems", *IEE Proceedings Control Theory and Applications*, vol. 149, No. 3, pp. 193-201, May 2002.
- [17] R. M. Sanner and J. E. Slotine, "Gaussian Networks for Direct Adaptive Control", *IEEE Trans. Neural Networks*, vol. 3, no. 6, pp. 837-863, Nov. 1992.
- [18] I. Ten and T. Hiroshi, "Simulation of the ocean waves and appearance of Freak waves", *Reports of RIAM Symposium*, no. 17SP1-2, no. 04, 2006.

REFERENCES

- [1] R. D. Eubank, E. M. Atkins and D. Macy, "Autonomous Guidance and Control of the Flying Fish Ocean Surveillance Platform", *Infotech@Aerospace Conference*, Seattle, Washington, Apr. 2009, AIAA-2009-2021.
- [2] R. D. Eubank, "Autonomous Flight, Fault, and Energy Management of the Flying Fish Solar-Powered Seaplane", Ph.D. dissertation, Aerospace Engineering, University of Michigan, 2012.
- [3] Y. Zhu, G. Fan and J. Yi, "Modeling longitudinal aerodynamic and hydrodynamic effects of a flying boat in calm water", *Proceedings of*